行政院國家科學委員會補助專題研究計畫成果報告

****
* 光纖通訊應用光電元件製作及數值模擬 — 子計畫三： *
* 半導體光放大器元件內非線性現象與放大自發放光雜訊之數值研究 *
****

計畫類別：整合型計畫

計畫編號：NSC 90-2215-E-002-029

執行期間：九十年八月一日至九十一年七月三十一日

計畫主持人：江衍偉，國立台灣大學電信工程學研究所

執行單位：國立台灣大學電信工程學研究所

中華民國九十一年十月八日

行政院國家科學委員會專題研究計畫成果報告

光纖通訊應用光電元件製作及數值模擬— 子計畫三：半導體光放大器元件內非線性現象與放大自發放光雜訊之數值研究

Numerical Studies on Nonlinear Phenomena and Amplified Spontaneous Emission Noise in Semiconductor-Optical-Amplifier Devices

計畫編號：NSC 90-2215-E-002-029
執行期間：九十年八月一日至九十一年七月三十一日
主持人：江衍偉，國立台灣大學電信工程學研究所
參與人員：王志洋、郭乃仁、林志南、王祥旭、陳弘基、劉貴朝，台灣大學電信所

摘要

我們以數值方法分析一多模干涉半導體光放大器之波長轉換效果。藉由時域行進波法與 Runge-Kutta 法，我們模擬了交互增益/相位調變等非線性現象，以探討此種波長轉換器的操作效率。吾人亦探討了輸入訊號上的可加性雜訊對輸出訊號的影響。
關鍵詞：波長轉換、交互增益/相位調變、多模干涉、半導體光放大器

Abstract

The performance of wavelength conversion in a multimode-interference semiconductor optical amplifier is numerically investigated. The nonlinear phenomena including cross-gain and cross-phase modulations were simulated using the time-domain traveling-wave model together with the Runge-Kutta method. Also studied are the effects of additive noise on the signal-to-noise ratio of wavelength conversion output.
Keywords: wavelength conversion, cross-gain/phase modulation, multimode-interference, semiconductor optical amplifiers

Because of the required functions of wavelength reuse and dynamic routing in a wavelength-division-multiplexing fiber communication network, all-optical wavelength conversion has been an issue of research focus for years. Besides four-wave mixing either in a semiconductor optical amplifier (SOA) [1] or in fiber [2], the most commonly used methods are based on cross-gain and/or cross-phase modulation in an SOA [3,4]. Recently, it has been experimentally and numerically shown that an SOA with a directional coupler configuration can improve the functions of wavelength conversion based on the cross-phase modulation [5,6]. The directionally coupled SOA scheme has advantages over a conventional SOA wavelength converter in several aspects, including extinction ratio and response speed.

In this study, we report the results of numerical studies on wavelength conversion based on cross-gain/phase modulation in a multimode-interference (MMI) SOA. Although an MMI SOA can be regarded as a directional coupler of zero gap and its linear coupling phenomenon is similar to that of a directional coupler, their nonlinear coupling behaviors based on gain saturation and the associated phase modulation can be different [7]. With our MMI SOA configuration, we found that the switching speed could be higher with about the same switching contrast, when compared with the operation in a directional coupler configuration. We also evaluated the effects of additive noise on the signal-to-noise ratio of wavelength conversion output.

The top view of the MMI SOA

wavelength converter is schematically shown in Fig. 1. Here, a modulated pump signal and a continuous-wave (CW) probe input are applied to the MMI SOA from bar port 1. The bar (cross) port is defined as the lower (upper) half of the MMI waveguide. In a real implementation, leading single-mode waveguides might be needed for input/output coupling. The number 1 (2) after either the bar port or cross port means the input (output) end. Through the cross-gain/phase modulation and the nonlinear coupling induced by gain saturation in the MMI SOA, the pulse-train pattern at the pump wavelength is then copied to the probe signal, exiting from cross port 2 or bar port 2.

To investigate the performance of the MMI SOA wavelength converter, we need to solve the problem of multimode wave propagation of light pulses at two wavelengths. Assume that at each wavelength, only two waveguide modes can be guided in the MMI SOA. It can be derived that the four slowly-varying complex mode amplitudes satisfy four coupled differential equations [7]. Also, the carrier density as well as the gain constant satisfies a rate equation, which is nonlinearly related to the coupled wave equations. For numerical computations, the MMI SOA was divided into small sections along the propagation direction with step size about 5 μm, and the time-domain traveling-wave method [7,8] was employed to solve the coupled wave equations. At each time instant, four complex amplitudes were evaluated in each section to obtain the fields at the next time instant. The total light intensity of each wavelength could be calculated and then substituted into carrier density rate equation, which was solved with the Runge-Kutta method to update the values of carrier density and hence gain constant. This newly obtained gain constant distribution was used to update the coefficients in coupled wave equations at the next time instant. After iterating the procedures, the output complex amplitudes and hence the optical intensities of both pump and probe signals through the MMI SOA could be obtained.

The pump and probe wavelengths were chosen to be 1.550 and 1.565 μm, respectively. Plotted in Figs. 2 (a) and (b) are the output pulse patterns of the probe power from cross port 2 and from bar port 2, respectively, with the MMI SOA length equal to 500 μm (larger than the coupling length 351 μm). Here, the input power of the square pump pulse was 0 dBm (-10 dBm) at level 1 (0) with bit rate at 10 Gbit/sec, and the input power of the probe wave was -30 dBm. The simulations show an extinction ratio about 9 (slightly smaller than the input extinction ratio 10) in cross port 2. It is noted that the response of wavelength conversion is quite fast with a time constant less than 100 psec. Such a fast response resulted in better waveforms in the two output ports, as compared with those in [6]. The risetime is longer than the falltime because the carrier recovery process takes a longer time. The associated frequency chirp, defined as the time derivative of the signal phase divided by 2π, in cross port 2 is shown in Fig. 2(c). One can see that the frequency chirp is more severe when the waveform is falling or rising. This is consistent with the fact that carrier density varies rapidly at these time instants. Again, the frequency chirp is smaller at intensity rise than at intensity fall because of the slow carrier recovery process.

In general, there are two kinds of noise affecting the performance of a wavelength converter. One is the additive noise associated with the input pump signal, coming from the pre-stage amplifiers [9]. The other is the amplified spontaneous emission noise, generated and amplified within the SOA [10]. It has been shown that the latter effect is usually much weaker than the former when the SOA is under saturation [11]. Here, we numerically investigate the effects of the additive noise on output probe signal through an MMI SOA of 500 μm in length. In simulations, the standard deviation of noise at pump signal level 1 was chosen ten times larger than that at pump signal level 0. Since the input pump power at level 1 was assumed 10 dB higher than that at level 0, the input signal-to-noise ratio (SNR) at level 1

was 10 dB lower than that at level 0. After generating realizations of random noise with various specific standard deviations, we first computed the input SNR. Shown in Fig. 3 are the variations of input SNR at level 1 (thick dashed curve) and at level 0 (thin dashed curve) versus the input noise standard deviation at level 1. Then, the noise contaminated pump signal together with the noise-free CW probe was fed into the MMI SOA through bar port 1. Using the aforementioned simulation algorithms, we can compute the probe output signal from cross port 2, and hence the output SNR. Also plotted in Fig. 3 are the variations of output SNR at level 1 (thick solid curve) and at level 0 (thin solid curve) versus the input noise standard deviation at level 1. In spite of the fluctuations, the output SNR is generally higher than the input level, except the case of high input SNR, where the input noise is too small to have a practical effect. Because carrier density cannot keep up with the random variation of noise, the MMI SOA acts like a low-pass filter suppressing the high-frequency portion of noise. Thus, the output SNR becomes higher than the input value.

In conclusion, we have shown the simulation results of wavelength conversion in an MMI SOA. Four wave equations for two modal amplitudes at the pump and probe wavelengths and a rate equation for carrier density were simultaneously solved using the time-domain traveling-wave model together with the Runge-Kutta method. With parameter values similar to those in [6], we found that high extinction ratios (about 10), better waveforms and a shorter response time (less than 100 psec) could be obtained with our MMI SOA wavelength converter. The effects of the additive noise have also been simulated with the results showing that the output SNR was generally higher than the input one.

References

1. M. C. Tatham, "20 nm optical wavelength conversion using nondegenerate four-wave-mixing," *IEEE Photon. Technol. Lett.*, vol. 5, pp. 1303-1306, 1993.
2. K. Inoue, "Polarization-insensitive wavelength conversion using fiber four-wave mixing with two orthogonal pumps at different frequencies," in Tech. Dig. *OFC '94*, San Jose, CA, Feb. 1994, paper THQ5.
3. A. D. Ellis, A. E. Kelly, D. Nesset, D. Pitcher, D. G. Moodie, and R.Kashyap, "Error free 100 Gb/s wavelength conversion using grating assisted cross gain modulation in a 2 mm long semiconductor amplifier," *Electron. Lett.*, vol. 34, pp. 1958–1959, 1998.
4. C. Joergensen, S. L. Danielsen, T. Durhuus, B. Mikkelsen, K. E. Stubkjaer, N. Vodjdani, F. Ratovelomanana, A. Enard, G. Glastre, D. Rondi, and R. Blondeau, "Wavelength conversion by optimized monolithic integrated Mach-Zehnder interferometer," *IEEE Photon. Technol. Lett.*, vol. 8, pp. 521-523, 1996.
5. B. Ma and Y. Nakano, "Realization of all-optical Wavelength converter based on directionally coupled semiconductor optical amplifiers," *IEEE Photon. Technol. Lett.*, vol. 11, pp. 188-190, 1999.
6. M. Saitoh, B. Ma, and Y. Nakano, "Static and dynamic characteristics analysis of all-optical wavelength conversion using directionally coupled semiconductor optical amplifiers," *IEEE J. Quantum Electron.*, vol. 36, pp. 984-990, 2000.
7. J. Y. Wang, J. H. Lee, Y. W. Kiang, and C. C. Yang, "Numerical simulation on pulsed operation of an all-semiconductor optical amplifier nonlinear loop device," *J. Lightwave Technol.*, vol. 19, 1768-1776, 2001.
8. L. M. Zhang, S. F. Yu, M. C. Nowel, D. D. Marcenac, J. E. Carrol and R. G. S. Plumb, "Dynamic analysis of radiation and side-mode suppression in a second-order DFB laser using time-domain large-signal traveling wave model," *IEEE J. Quantum Electron.*, vol. 30, pp. 1389-1395, 1994.

9. K. Inoue, "Noise transfer characteristics in wavelength conversion based on cross-gain saturation in a semiconductor optical amplifier," *IEEE Photon. Technol. Lett.*, vol. 8, pp. 888-890, 1996.
10. D. Cassioli, S. Scotti, and A. Mecozzi, "A time-domain computer simulator of the nonlinear response of semiconductor optical amplifiers," *IEEE J. Quantum Electron.*, vol. 36, pp. 1072-1080, 2000.
11. S. I. Pegg, M. J. Fice, M. J. Adams, and A. Hadjifotiou, "Noise in wavelength conversion by cross-gain modulation in a semiconductor optical amplifier," *IEEE Photon. Technol. Lett.*, vol. 11, pp. 724-726, 1999.

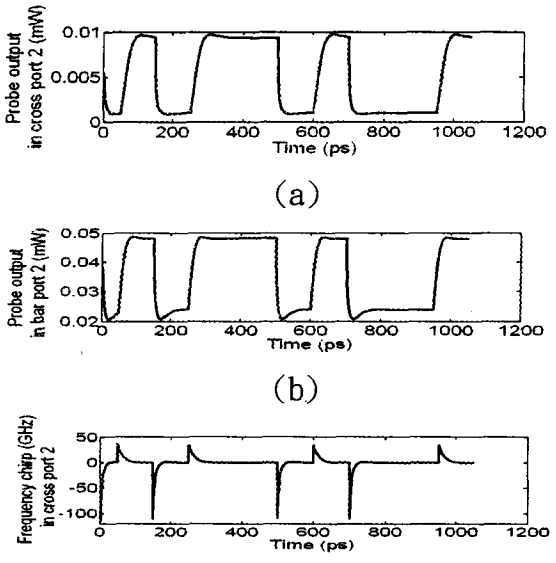

Fig. 2 Output patterns of the power from cross port 2 (a), power from bar port 2 (b), and frequency chirp from cross port 2 (c) when the length of the MMI SOA is 500 μm.

Fig. 1 Schematic of an MMI SOA wavelength converter

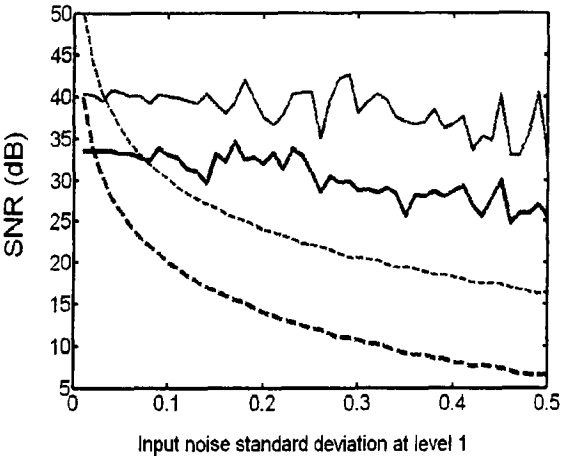

Fig. 3 Input and output SNR values versus input noise standard deviation at level 1: thick dashed curve for input at level 1; thick solid curve for output at level 1; thin dashed curve for input at level 0; thin solid curve for output at level 0. The length of the MMI SOA is 500 μm.